Journal of Computational Neuroscience 18, 255–263, 2005

Coexistence of Tonic Spiking Oscillations in a Leech Neuron Model

GENNADY CYMBALYUK
Department of Physics and Astronomy, Georgia State University, Atlanta, GA 30303, USA
gcym@phy-astr.gsu.edu

ANDREY SHILNIKOV
Department of Mathematics and Statistics, Georgia State University, Atlanta, GA 30303, USA
ashilnikov@gsu.edu

Received January 6, 2005; Revised January 18, 2005; Accepted January 19, 2005

Abstract. The leech neuron model studied here has a remarkable dynamical plasticity. It exhibits a wide range of activities including various types of tonic spiking and bursting. In this study we apply methods of the qualitative theory of dynamical systems and the bifurcation theory to analyze the dynamics of the leech neuron model with emphasis on tonic spiking regimes. We show that the model can demonstrate bi-stability, such that two modes of tonic spiking coexist. Under a certain parameter regime, both tonic spiking modes are represented by the periodic attractors. As a bifurcation parameter is varied, one of the attractors becomes chaotic through a cascade of period-doubling bifurcations, while the other remains periodic. Thus, the system can demonstrate co-existence of a periodic tonic spiking with either periodic or chaotic tonic spiking. Pontryagin's averaging technique is used to locate the periodic orbits in the phase space.

Keywords: Pontryagin's averaging method, chaos, chaotic tonic spiking, bi-stability, bifurcation, transition, period-doubling

1. Introduction

Neurons can be viewed as strongly non-linear dynamical systems capable of generating complex patterns of activity. A ubiquitously observed pattern is tonic spiking. Tonically spiking neurons have been related to different functions of the nervous system, such as coding of sensory information, information processing, memory formation, attention and motor control (Gray and Singer, 1989; Bazhenov et al., 2000; Hoppensteadt and Izhikevich, 1998; Marder and Calabrese, 1996; Marder et al., 1996; Vinogradova, 2001; Borisyuk and Kazanovich, 2004; Hounsgaard and Kiehn, 1989; Schwarz and Thier, 1999; Hopfield and Brody, 2001).

Neurons can exhibit multistability of activity like bursting and tonic spiking as well as rest states. In terms of dynamical systems, multi-stability means coexistence of several attractors in the phase space of a system. The particular attractor (mode) exhibited by the neuron is determined by initial conditions. The initial conditions of the model represent membrane potential and the states of the ion conductances. The multistability of activity modes has been observed in modelling studies (Bertram, 1993; Canavier et al., 1993; Cymbalyuk and Calabrese, 2001) and neurophysiological experiments (Hounsgaard and Kiehn, 1989; Lechner et al., 1996; Turrigiano et al., 1996). It sets a remarkable framework for potential dynamical plasticity of neurons with implications for dynamical memory, information processing and motor control (Canavier et al., 1993; Turrigiano et al., 1996; Marder et al., 1996; Hounsgaard and Kiehn, 1989; Hoppensteadt and

Izhikevich, 1998). In a model, multistability may occur within a specific parameter range. Neuromodulators can alter drastically the dynamics of the neuron and it is plausible to suggest that they play an important role in control of the multistability (Canavier et al., 1994).

The coexistence of tonic spiking modes in neurons has been experimentally demonstrated in Lechner et al. (1996). Here we explain how this kind of bi-stability can occur in a model of a leech neuron. We study the model of a leech neuron under specific pharmacological conditions such that all known currents, but the transient sodium current and non-inactivating potassium current, are blocked. This model possesses rich dynamics and shows a variety of different activities. Our previous studies demonstrated that this model could explain long plateau-like oscillations, observed in leech neurons under these pharmacological conditions (Cymbalyuk and Calabrese, 2001). Under different parametric conditions it can also show tonic spiking activity, bursting or silence. Recently, we have reported and analyzed two novel scenarios of transition between tonic spiking and bursting (Shilnikov et al., 2004, 2005a, b). One of these scenarios (Shilnikov et al., 2005a) describes a smooth and reversible transition between tonic spiking and bursting. The other (Shilnikov et al., 2004, 2005b) explains the co-existence of bursting and tonic spiking modes which are separated by a saddle periodic orbit. This mechanism is based on a Lukyanov-Shilnikov bifurcation for a saddle-node periodic orbit with non-central homoclinic orbits. To locate these periodic orbits and study their bifurcations we developed a geometrical framework for Pontryagin's averaging method of singularly perturbed systems. Here we report the conditions under which this model demonstrates another kind of bi-stability with two coexistent tonic spiking modes. The developed averaging technique gives us a clear geometrical interpretation of the phenomenon. Moreover, as a bifurcation parameter is varied we can observe the evolution of one of the tonic spiking regimes from periodic spiking through a cascade of period-doubling bifurcations into the chaotic tonic spiking mode.

2. Model

Here we employ our previously developed model of a leech neuron under certain pharmacological conditions (Cymbalyuk and Calabrese, 2001). It is based on the canonical model of identified leech oscillator interneurons that are part of the leech heartbeat central pattern generator (Hill et al., 2001). It utilizes dynamics of the seven voltage-dependent ionic currents quantified in the voltage-clamp experiment and incorporated into a system of differential equations through Hodgkin-Huxley formalism, see (Hill et al., 2001; Opdyke and Calabrese, 1994) and references therein. In addition to these currents, the model adopts the transient sodium current from the original work by Hodgkin and Huxley (1952). The canonical model has been shown to replicate the activity of the leech oscillator interneurons under different pharmacological conditions and treatments (Hill et al., 2001; Cymbalyuk and Calabrese, 2001; Cymbalyuk et al., 2002). The complete, canonical neuron model appears to be quite a challenge for a comprehensive analysis. For the reason of simplicity we use the pharmacologically reduced model. It represents the activity of the single neuron under pharmacological conditions such that all Ca currents, hyperpolarization-activated current, persistent, non-inactivating sodium current and two potassium currents, a delayed rectifier-like potassium current and a fast transient potassium current, are blocked, while a persistent potassium current (I_{K2}) is partially blocked.

Our simplified model, based on the dynamics of I_{Na} and I_{K2} currents, is described by a system of the following three differential equations:

$$\begin{aligned} C\dot{V} &= -\big(\bar{g}_{K2}\, m_{K2}^2 (V - E_K) + g_l\,(V - E_l) \\ &\quad + \bar{g}_{Na} f(-150, 0.0305, V)^3 h_{Na}(V - E_{Na})\big), \\ \dot{m}_{K2} &= \frac{f\big(-83, 0.018 + V_{K2}^{shift}, V\big) - m_{K2}}{\tau_{K2}}, \\ \dot{h}_{Na} &= \frac{f(500, 0.0333, V) - h_{Na}}{\tau_{Na}}, \end{aligned} \tag{1}$$

where the variables V, m_{K2}, and h_{Na} are the membrane potential, activation of I_{K2} and inactivation of I_{Na}, respectively. The parameters are: C is the membrane capacitance, $\bar{g}_{K2}$ is the maximum conductance of I_{K2}; E_K and E_{Na} are the reversal potentials of K^+ and Na^+, respectively; $\bar{g}_{Na}$ is the maximal conductance of I_{Na}; g_l and E_l are the conductance and reversal potential of the leak current, respectively; τ_{K2} and τ_{Na} are the time constants of activation of I_{K2} and inactivation of I_{Na}, respectively; V_{K2}^{shift} is the shift of the membrane potential of half-activation of I_{K2} from its

canonical value. The function f is a Boltzman function: $f(A, B, V) = 1/(1 + e^{A(B+V)})$. The values of the parameters used in this study are $C = 0.5$ nF, $\bar{g}_{K2} = 30$ nS, $E_K = -0.07$ V, $E_{Na} = 0.045$ V, $\bar{g}_{Na} = 200$ nS, $g_l = 8$ nS, $E_l = -0.046$ V, $\tau_{K2} = 0.25$ sec and $\tau_{Na} = 0.0405$ sec. We use V_{K2}^{shift} as a bifurcation parameter.

3. Finding Periodic Orbits

In the model (1), the activation of I_{K2} is almost ten times slower than V and the inactivation of I_{Na}. Hence, we may treat it as the slow state variable. The other variables,V and h_{Na}, will be treated as the fast state variables. Thus, we can view (1) as a singularly perturbed system that is recast in the following appropriate form:

$$\dot{\mathbf{x}} = \mathbf{f}(\mathbf{x}, z) \quad \dot{z} = \mu[g(x, \alpha) - z], \tag{2}$$

where $\mathbf{x} = (x, y)$ and $z \in R^1$, α is a single control parameter, and $0 < \mu \ll 1$. Since the rate of change of the z-variable is much smaller than that of $\mathbf{x}$, the equations in (2) are called fast and slow subsystems, respectively. In terms of the model (1), $x \equiv V$, $y \equiv h_{Na}$, $z \equiv m_{K2}$ and $\alpha \equiv V_{K2}^{shift}$.

Let the functions, $\mathbf{f}$ and g, be smooth enough. Note that the way the righthand side of the slow equation is written is quite typical for neuron models of the Hodgkin-Huxley type. The surfaces, $\mathbf{f}(\mathbf{x}, z) = 0$ and $z = g(x, \alpha)$, are called the nullclines, fast and slow, respectively. By varying α, we can move the slow nullcline in the phase space of the system. Let its projection onto the (z, x)-plane have a typical logarithmic shape like a biophysically realistic one in a Hodgkin-Huxley-type model. This slow nullcline will be labelled as $\dot{z} = 0$ in Fig. 1. It states the fact that the z-component of the vector field generated by Eqs. (2) equals to zero on it. Above the slow nullcline, the z-component of the vector field is oriented rightward because $\dot{z} > 0$, and leftward underneath it where $\dot{z} < 0$. In the projection onto the (z, x)-space, the fast nullcline (M_{eq} in Fig. 1) has a distinct Z-shape with the two knee points at z_{sn}^1 and z_{sn}^2. When $\mu = 0$, the slow z-variable becomes a parameter in the independent fast subsystem. By varying z, one can trace the curve of equilibria of the fast subsystem. Its knee point corresponds to a saddle-node bifurcation where two equilibrium states merge and annihilate themselves. The lower branch of the fast nullcline, which corresponds to the hyperpolarized state of the neuron, is formed by stable equilibria of the fast subsystem. The middle one consists of saddles, and the upper branch, which corresponds to the depolarized state of the neuron, consists of totally unstable equilibria of the fast subsystem.

The upper branch is surrounded by a cylindric surface M_{lc} comprised of the stable, M_{lc}^s, and unstable, M_{lc}^u limit cycles of the fast subsystem, see Fig. 1. The surface M_{lc} has an edge at z_{sn}^{lc} where both branches merge, which corresponds to a saddle-node bifurcation of the limit cycles of the fast subsystem.

Let us consider the full system at small $\mu \neq 0$. An equilibrium state of (2) lies in the intersection of the fast and slow nullclines. When the slow nullcline crosses transversally the hyperpolarized branch of the Z-shaped fast nullcline from below, the equilibrium state, which is already stable in the $\mathbf{x}$-subspace, is stable in the z-direction as well. This is because the intersection point divides the stable hyperpolarized branch so that to the right of the point, $\dot{z} < 0$ in M_{eq}, and $\dot{z} > 0$ on the left of it. As α is varied, the intersection point moves along the nullcline M_{eq}. Let the slopes of both the nullclines be such that there is a single intersection point. However, this equilibrium state may change its stability when the slow nullcline $\dot{z} = 0$ passes through the left knee point at z_{sn}^1. Observe that at this point the equilibrium state of the full system at $\mu = 0$ has two zero characteristic exponents. When $0 < \mu \ll 1$, the slow and fast equations are linked, and so are the characteristic exponents of the equilibrium state residing near the fold. The characteristic exponents become complex conjugates remaining close to the origin in the complex plane. Their real part is negative when the equilibrium state is on the hyperpolarized branch, but becomes positive when the points move onto the middle branch of M_{eq}. Therefore, just as the equilibrium state passes through the knee point, it losses its stability through an Andronov-Hopf bifurcation, which can be either super- or sub-critical. A small amplitude stable or unstable periodic orbit emerges from or collapses into the equilibrium state respectively. It is shown in Arnold et al. (1994), that the type of criticality, i.e. sub- or super-, of this bifurcation in a singularly perturbed system is determined by the sign of $\mathbf{f}'''$ at a fold in approximation of $\mu = 0$. This criterion is extremely simple and easily applicable for all neuron models of the considered type. After the bifurcation, the equilibrium state becomes a saddle-focus with a two-dimensional unstable manifold and one dimensional stable manifold. The latter is due to a third characteristic exponent

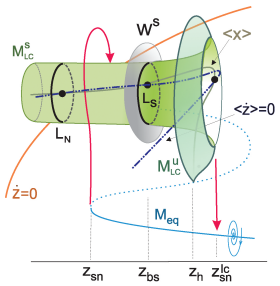

Figure 1. Bifurcation diagram of the fast subsystem in the $(z, \mathbf{x})$-phase space. Here, $M_{\rm eq}$ and $M_{\rm lc}$ are the α-parametric manifolds comprised of equilibria and periodic orbits, respectively. The intersection point of the slow nullcline, $\dot{z} = 0$ and $M_{\rm eq}$, yields an unstable equilibrium state; curves $\langle x \rangle$ and $\langle \dot{z} \rangle = 0$ are the average nullclines. Their three intersection points correspond to three periodic orbits: stable L_n and saddle L_s on the attracting branch $M^s_{\rm lc}$, and one of undetermined stability that lies on the unstable branch $M^u_{\rm lc}$. The latter is foliated by the repelling limit cycles of the fast subsystem. The stable manifold W^s of the saddle orbit bounds the attraction basin of L_s corresponding to the periodic tonic spiking in the neuron system. Compare this figure with the phase portrait of the neuron model (1) shown in Fig. 2.

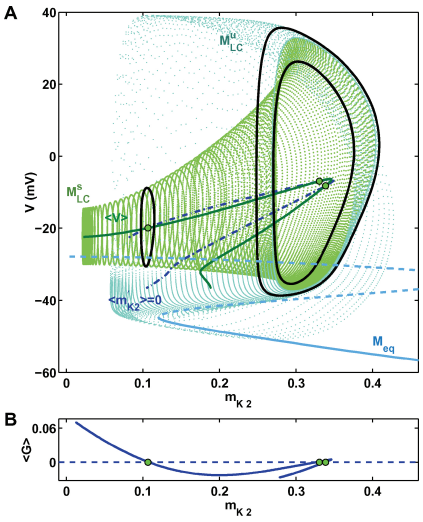

Figure 2. Numerical phase portrait of the neuron model (1) and the bifurcation diagram of its fast subsystem (A) and the graph of the function $\langle G(m_{\rm K2}) \rangle$ (B) for $V^s_{\rm K2} = -0.0254$ V. The blue z-shaped line, $M_{\rm eq}$, consists of the equilibrium states of the fast subsystem (dotted and solid segments represent unstable and stable ones). The green cylinder-shaped surface $M_{\rm lc} = M^s_{\rm LC} \cup M^u_{\rm LC}$ is comprised of the stable and unstable limit cycles of the fast subsystem. The line $\langle V \rangle$ shows the dependence of the V-coordinate of the limit cycle averaged over its period on $m_{\rm K2}$. The dashed, blue line is the average nullcline $\langle \dot{m}_{\rm K2} \rangle = 0$. The intersection points of $\langle V \rangle$ and $\langle \dot{m}_{\rm K2} \rangle = 0$ correspond to the periodic orbits presented by black solid closed curves. (B) The sign of the derivative $\langle \dot{G} \rangle|_{z_0}$ determines the stability of this periodic orbit in the $m_{\rm K2}$-direction. It is stable when the derivative is negative (the left point), and unstable when it is positive (the middle and right points).

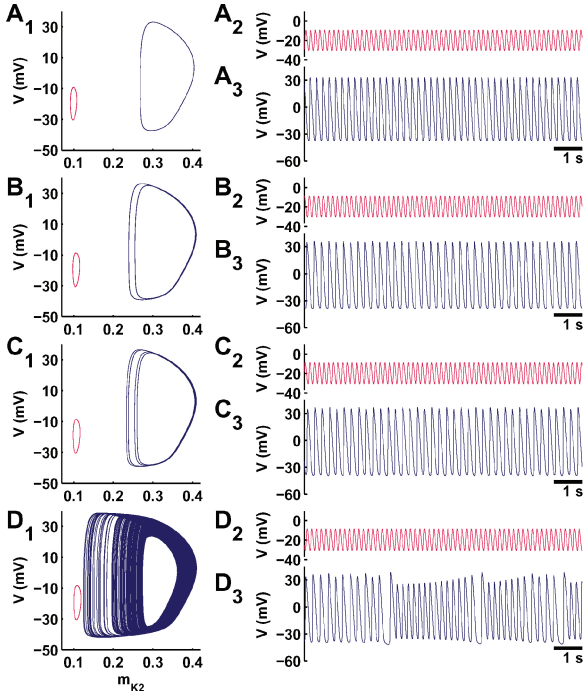

Figure 3. Bi-stability of two tonic spiking attractors for the different values of $V^{\rm shift}_{\rm K2}$: (A) $V^{\rm shift}_{\rm K2} = -0.026V$, (B) $V^{\rm shift}_{\rm K2} = -0.02555V$, (C) $V^{\rm shift}_{\rm K2} = -0.0255V$, (D) $V^{\rm shift}_{\rm K2} = -0.025361V$. The smaller amplitude spiking does not change much as the parameter is varied (A_2, B_2, C_2, D_2), while the larger amplitude spiking undergoes a series of period-doubling bifurcations. Initial conditions are provided in the Appendix.

which is negative. Recall that in the restriction to the subspace of the fast subsystem at $\mu = 0$, the given equilibrium state is a saddle. Following the terminology of Shilnikov et al. (1998, 2001), we emphasize that the point is a saddle-focus not because it has a pair of complex exponents but because this pair is closer to the imaginary axes in the complex plane than its third negative exponent. This implies that shall the saddle-focus possess a homoclinic orbit, the fulfilment of the Shilnikov conditions is guaranteed (in the backward time). Hence, the system should have a chaotic set with narrow islands containing weakly stable periodic orbits. This follows from the fact that the divergence of the vector field is negative.

As the equilibrium state climbs the middle branch of $M_{\rm eq}$ up further away from the fold, its characteristic exponents become real and distinct. One characteristic exponent of this simple saddle remains positive and small, of order μ (it is due to the contribution of the slow subsystem) while the other two are large and of

opposite signs. This means that if one of its two stable one-dimensional separatrix of the saddle becomes homoclinic to it, only a saddle periodic orbit may emerge from the loop. These conditions ensure that no stable periodic orbit may emerge as a result of a homoclinic bifurcation of such a saddle of the full system. As far as homoclinic bifurcations of its fast subsystem are concerned, the problem is also reduced to evaluating the sign of the saddle-value, which is a sum of the positive and negative characteristic exponents of the 2D saddle. By the proposed construction, this saddle value is to be positive in our case, which means that only a repelling limit cycle emerges from this bifurcation at z_h. As the parameter is increased, this unstable limit cycle traces out the surface $M^u_{\rm lc}$, then meets the stable limit cycle at $z^{\rm lc}_{\rm sn}$ and vanishes. Let such a periodic solution of the fast subsystem be given by $\mathbf{x} = \varphi(t, z)$ of period $T(z)$. The exponential stability of the limit cycle is determined by the magnitude of the single positive Floquet multiplier

$$\rho_1(z) = e^{\int_0^{T(z)} Div\, \mathbf{f}(\varphi(t,z))\, dt}. \tag{3}$$

If it is strictly inside of a unit circle, then the limit cycle is exponentially stable, otherwise it is repelling. The other multiplier of the limit cycle is always $+1$ because it corresponds to the zero Lyapunov characteristic exponent along the cycle (Shilnikov et al., 1998, 2001). Observe from (3) that a saddle-node bifurcation occurs when the multiplier ρ_1 of the half-stable limit cycle equals one, i.e. the average divergence of the vector field on this orbit equals zero.

Let the slow nullcline $\dot z = 0$ pass underneath the surface $M^s_{\rm lc}$ in the phase space of system (2) at $0 < \mu \ll 1$ and intersect the middle segment of fast nullcline $M_{\rm eq}$. In this case a bursting activity is observed (Cymbalyuk and Calabrese, 2001; Shilnikov et al., 2004, 2005a) of "fold/fold cycle" type according to the classification suggested in Izhikevich (2000). A neighboring trajectory gets attracted to this cylinder-shaped surface so that it starts coiling around $M^s_{\rm lc}$ while translating rightwards. This part of the trajectory is the spiking phase of bursting waveform. Having reached the fold of the surface $M_{\rm lc}$ the phase point falls down to the hyperpolarized state and moves leftward. This part of trajectory is the quiescent phase of bursting. Then, the phase point returns to the spiking phase after passing the left knee point of the curve $M_{\rm eq}$ and thus completes the bursting cycle.

However, if the nullcines intersect, the situation becomes less clear. Namely, while the phase point moves about the surface $M_{\rm lc}$ above the nullcline $\dot z = 0$, its z-component increases so that the point translates slowly to the right. However, when it moves below the slow nullcline, the vector field pushes it to the left because here $\dot z < 0$. If these factors cancel each other out, the z-component of the phase point stays the same on average, and the phase point repeats the path over and over again. As a result, a periodic orbit of the full system is born near the surface $M_{\rm lc}$. To draw a parallel with the evolution of the equilibrium states described above, below we introduce a slow, "average" nullcline $\langle \dot z \rangle = 0$ as follows. It comes from Pontryagin and Rodygin (1960) that the overall normalized contribution of the slow subsystem on the trajectory on $M_{\rm lc}$ is given by

$$\langle G(z;\alpha)\rangle = \mu\left[\frac{1}{T(z)}\int_0^{T(z)} g(\mathbf{x}(t;z),\alpha)\, dt - z\right] \equiv \langle \dot z\rangle. \tag{4}$$

One can see that this "averaged" equation describes the dynamics of the z-component of trajectories on $M_{\rm lc}$. After integration, we obtain a function $\langle G(z)\rangle$ of a single variable z. The domain of this double-valued function is defined by the range of $M_{\rm lc}$. By construction, a zero z_0 of $\langle G(z)\rangle$ is an equilibrium state of the system (4) and hence corresponds to a periodic orbit of the full system. The sign of the derivative $\langle \dot G\rangle|_{z_0}$ determines the stability of this periodic orbit in the z-direction (Fig. 2B). It is stable when the derivative is negative, and unstable when it is positive. The periodic orbit of the full system corresponding to a zero is stable if it lies in the intersection of the plane $z = z_0$ and the stable branch $M^s_{\rm lc}$. Otherwise, if $\langle \dot G\rangle|_{z_0} > 0$, the periodic orbit is of saddle type. It has two two-dimensional manifolds, stable W^s and unstable W^u. Locally, the unstable manifold W^u is a cylinder which is a part of $M^s_{\rm lc}$. The stable manifold of a saddle periodic orbit is formed by the trajectories that converge to the orbit in the forward time. If μ is small enough, then the plane tangent to W^s is given by $z = z_0$. When $z_h < z_0 < z^{\rm lc}_{\rm sn}$, there is another periodic orbit on the unstable branch $M^u_{\rm lc}$. It is an unstable, either saddle or repelling, periodic orbit depending on the sign of the derivative $\langle \dot G\rangle|_{z_0}$.

Thus, if there are two simple zeros ($\langle \dot G\rangle|_{z_0} \neq 0$), then there are two periodic orbits on the manifold $M^s_{\rm lc}$: stable L_n and saddle L_s. The stable manifold of the saddle periodic orbit bounds the attraction basin of the stable one. This periodic attractor represents observable periodic tonic spiking activity of the neuron, see Figs. 2 and 3.

Also, the system can demonstrate bi-stability, if there is a second attractor. In the next section, we discuss possible scenarios of its formation and the role of the third periodic orbit in it.

3.1. Average Nullclines

To make the idea of Pontryagin's averaging technique more illustrative, let us introduce the notion of the average nullclines. For the sake of simplicity, suppose that the function $g(x, \alpha)$ is linear, i.e. the slow nullcline is a straight line. Variation of α governs either its slope or translates it in (z, x)-plane. Let the system (2) have a periodic orbit on $M_{\rm lc}$ at some α, which lies in the plane $z = z_0(\alpha)$, then the average value of its fast x-coordinate can be defined as $\langle x(\alpha)\rangle = \frac{1}{T(z)} \int_0^{T(z)} \varphi(t; z(\alpha))\, dt$. So, by varying α, a parametric curve $(z_0(\alpha), \langle x(\alpha)\rangle)$ can be defined. This curve is labelled $\langle x\rangle$ and $\langle V\rangle$ in Figs. 1 and 2, respectively. Note that it has an easily recognizable fold point and terminates at the homoclinic bifurcation on the middle branch of the fast Z-shaped nullcline. It is worth noticing that the shape of the curve $\langle x\rangle$ does not depend on the choice of the shape of the slow nullcline.

By introducing

$$\langle g(\alpha)\rangle = \frac{1}{T(z)} \int_0^{T(z)} g(\varphi(t; z(\alpha)))\, dt, \qquad (5)$$

we can define the slow averaged nullcline as follows: it is a parametrically set curve $(\langle g(\alpha)\rangle, \langle x(\alpha)\rangle)$. Observe that $\langle g\rangle = C(\alpha) \cdot \langle x\rangle$, where $C(\alpha)$ is the slope of the nullcline $\dot{z} = 0$. In other words, in the linear case, the slow average nullcline coincides with the slow nullcline.

Typically, since the function on the righthand side of the slow subsystem is not linear, the shape of the averaged slow nullcline can be strongly nonlinear as well and thus can differ from the slow nullcline, as shown in Fig. 2 where it is labelled by $\langle \dot{m}_{\rm K2}\rangle = 0$. Observe that the slow average nullcline and $\langle V\rangle$ has the same range in the second variable by construction. An intersection point of both curves is a sought zero of (4) provided it occurs at the same α. Note that the overlapping may occur at different values of the parameter α, see Fig. 1; the same is true for the neuron model (1) whose nullclines are shown in Fig. 2.

Assume that variation of the parameter α preserves the first two intersections on the left, i.e. the stable L_n and saddle L_s periodic orbits persist. The stable orbit represents the periodic tonic spiking in the neuron. If there are no intersection points on $M^s_{\rm lc}$ within $z^1_{\rm sn} < z < z^{\rm lc}_{\rm sn}$, then this attracting cylindrical manifold becomes transient for the trajectories of the system. This supports the bursting activity. Such behavior may take place when the periodic orbits vanish off the manifold $M^s_{\rm lc}$ through the saddle-node bifurcation. Depending on the global structure of the bifurcation, two distinct scenarios are possible (Shilnikov et al., 2004, 2005a). In the first case, the tonic spiking is replaced by the bursting as a result of the blue sky catastrophe. This transition is smooth and reversible. Its key signature is that the bursting is periodic, and, moreover, burst duration is regulated as $1/\sqrt{\alpha - \alpha^*}$, where α^* is the critical parameter value. In the second case, where the saddle-node periodic orbit has noncentral homoclinics, the transition is characterized by bi-stability of co-existent tonic spiking and bursting modes. Also, in contrast to the former case, the duration of the bursting is estimated as $|1 \log /(\alpha - \alpha^*)|$. Furthermore, the bursting can be weakly chaotic (Shilnikov et al., 2005b).

Here, we report that in the neuron model (1) the averaged nullclines may indeed intersect three times, as shown in Fig. 2. The third intersection point may correspond to another stable periodic orbit, as long as it belongs to the upper branch of the curve $\langle x\rangle$. This periodic orbit is unstable when the intersection point is on the low branch of the curve $\langle x\rangle$ below the fold point.

Recall that the only way a stable periodic orbit may become repelling is through the secondary Andronov-Hopf bifurcation, also called the torus bifurcation. Note that the torus bifurcation may not occur in a 3D system with the sign-constant divergency. This condition may not be fulfilled near the fold of the manifold $M_{\rm lc}$ as follows from (3) provided that the contribution of the slow subsystem into the divergency is small when $|\mu| \ll 1$. This yields that another multiplier of the periodic orbit is close to $+1$ as well. This torus can be called a Hopf-initiated canard (Guckenheimer et al., 2000), as it is extremely thin and breaks down quickly thereby leading to the onset of chaos (Shilnikov and Rulkov, 2003, 2004; Shilnikov et al., 2004). As a parameter governing the averaged slow nullcline is changed, a pair of complex-conjugate multipliers with a positive real part, cross the unit circle inwards while the 2D torus collapses and the periodic orbit regains stability. So, by lowering the slow averaged nullcline $\langle \dot{z}\rangle = 0$, the third intersection point slips towards the the homoclinic bifurcation of the saddle equilibrium state on the

middle branch of $M_{\rm eq}$. It follows from the discussion above that no stable, but saddle periodic orbit can terminate at this homoclinic orbit. Therefore, the stable periodic orbit undergoes some evolution to become of saddle type.

The presence of the two stable periodic orbits in the phase space means bi-stability of tonic spiking activities of the neuron model, see Fig. 3A. The attraction basins of both the attractors are separated by the stable manifold of the saddle periodic orbit. This remains true even when the second periodic orbit becomes a saddle through a period-doubling bifurcation, see Fig. 3. After the bifurcation its stability is inherited by a stable periodic orbit of the doubled period (Fig. $3B_1$ and B_2). In turn, the stable orbit of doubled period loses its stability through a consequent period-doubling bifurcation so that a stable periodic orbit of period four is born (Fig. $3C_2$) and so forth. This gives rise to a period-doubling cascade leading to chaos (Fig. 3D). Thus, the model can demonstrate coexistence of two tonic spiking modes. One is always periodic, the other can be either periodic or chaotic depending on the value of the control parameter (Fig. 3). There are two cases of how a chaotic tonic spiking attractor may vanish. In the first case, it undergoes an internal crisis when its trajectories reach the fold of the manifold $M_{\rm lc}$ and fall down onto the hyperpolarized branch $M_{\rm eq}$ that tunnels them into the attraction basin of the primary periodic tonic spiking attractor. In the second case, the trajectories of the chaotic attractor start deserting through the separating saddle periodic orbit when the chaotic attractor on $M^u_{\rm lc}$ touches the stable manifold of the saddle periodic orbit. In either case, after the chaotic attractor has vanished, the system becomes mono-stable so that the periodic tonic spiking activity is observed for most initial conditions.

4. Conclusions

Bi-stability of tonic spiking has been observed in neurophysiological experiments (Lechner et al., 1996). Here we found bi-stability of tonic spiking in the model of leech oscillatory interneurons. We have shown that this model (1) can demonstrate bi-stability where two types of tonic spiking activity co-exist. Under control parameter variation one tonic spiking mode stays always periodic while the other undergoes a complex evolution so that it ranges from periodic to chaotic, experiencing a cascade of period-doubling bifurcations.

This cascade is one of the typical routes to chaos. The period-doubling cascade has been frequently observed in various neuron models (Terman, 1992; Feudel et al., 2000; Rowat and Elson, 2004; Wang, 1993; Rinzel and Ermentrout, 1989). A distinction of the model under consideration is that the chaotic attractor represents a co-existent alternative to the periodic tonic spiking activity. The period-doubling cascade is also a characteristic feature for transitions from tonic spiking into bursting described in Terman (1992), Feudel et al. (2000), Rowat and Elson (2004), Wang (1993), and Rinzel and Ermentrout (1989).

Pontryagin's averaging method provides us with a clear geometrical interpretation of the bi-stability phenomenon for the case of coexisting oscillatory modes. The mechanism which we present here differs from bi-stability reported in the same model (Shilnikov et al., 2005a, b) where a periodic tonic spiking and a bursting activities co-exist. Similarly to the bi-stability considered in Shilnikov et al. (2004, 2005b), the system has several periodic orbits and two of them directly correspond to the stable periodic orbit and the unstable periodic orbit of saddle type. In our previous work (Shilnikov et al., 2004) the unstable periodic orbit separates the basins of attraction of two co-existing modes: the tonic spiking periodic orbit and bursting regime. Here, it separates two modes in a similar fashion, except it has a tonic spiking regime coexisting with another spiking regime rather than with a bursting regime.

Appendix

The initial conditions for the two tonic spiking regimes presented in Fig. 3 are provided in the form (V, $m_{\rm K2}$, $h_{\rm Na}$) as follows:

(A) $V^{\rm shift}_{\rm K2} = -0.026V$, for (A_2) and (A_3) the initial conditions are $(-0.0293215,\ 0.0955228,\ 0.0997786)$ and $(0.0259645, 0.356993, 0.197492)$ respectively;

(B) $V^{\rm shift}_{\rm K2} = -0.02555V$, for (B_2) and (B_3) the initial conditions are $(-0.00893104,\ 0.103985,\ 0.0380690)$ and $(-0.0353596,\ 0.331244,\ 0.200898)$ respectively;

(C) $V^{\rm shift}_{\rm K2} = -0.0255V$, for (C_2) and $(C_3)$the initial conditions are $(-0.0179769,\ 0.0986789,\ 0.0683255)$ and $(-0.0227637,\ 0.370310,\ 0.0182421)$ respectively;

(D) $V_{K2}^{shift} = -0.025361V$, for (D_2) and (D_3) $(-0.0252204,\ 0.115693,\ 0.00855340)$ and $(-0.0376925,\ 0.297170,\ 0.524276)$ respectively.

Acknowledgment

The numeric analysis of the periodic solutions of system (1) is based on CONTENT (CONTENT) A.S. acknowledges the RFBR grants No. 02-01-00273 and No. 01-01-00975. G.C. was supported by NIH grants NS43098. A.S and G.C. appreciate a GSU internal research team and Brains & Behaviors research initiative grants.

References

Arnold VI, Afrajmovich VS, Ilyashenko YuS, Shilnikov LP (1994) Bifurcation Theory, Dynamical Systems V. Encyclopaedia of Mathematical Sciences. Springer-Verlag.

Bazhenov M, Timofeev I, Steriade M, Sejnowski TJ (2000) Spiking-bursting activity in the thalamic reticular nucleus initiates sequences of spindle oscillations in thalamic networks. J. Neurophysiology 84: 1076–1087.

Bertram R (1993) A computational study of the effects of serotonin on a molluscan burster neuron. Biol. Cybern. 69: 257–267.

Borisyuk RM, Kazanovich YB (2004) Oscillatory model of attention-guided object selection and novelty detection. Neural Netw. 17: 899–915.

Canavier CC, Baxter DA, Clark L, Byrne J (1993) Nonlinear dynamics in a model neuron provide a novel mechanism for transient synaptic inputs to produce long-term alterations of postsynaptic activity. J. Neurophysiol. 69: 2252.

Canavier CC, Baxter DA, Clark JW, Byrne JH (1994) Multiple modes of activity in a model neuron suggest a novel mechanism for the effects of neuromodulators. Multiple modes of activity in a model neuron suggest a novel mechanism for the effects of neuromodulators. J. Neurophysiol. 72: 872–882.

Cymbalyuk GS, Calabrese RL (2001) A model of slow plateau-like oscillations based upon the fast Na^+ current in a window mode. Neurocomputing 38–40: 159–166.

Cymbalyuk GS, Gaudry Q, Masino MA, Calabrese RL (2002) A model of a segmental oscillator in the leech heartbeat neuronal network. J. Neuroscience 22: 10580.

Feudel U, Neiman A, Pei X, Wojtenek W, Braun H, Huber M, Moss F (2000) Homoclinic bifurcation in a Hodgkin-Huxley model of thermally sensitive neurons. Chaos 10(1): 231–239.

Gray CM, Singer W (1989) Stimulus-specific neuronal oscillations in orientation columns of cat visual cortex. Proc. Natl. Acad. Sci. USA. 86: 1698–1702.

Guckenheimer J, Hofman K, Weckesserand W (2000) Numerical computations of canards. Int. J. Bifurcation and Chaos 2: 2669–2689.

Hill A, Lu J, Masino M, Olsen O, Calabrese RL (2001) A model of a segmental oscillator in the leech heartbeat neuronal network. J. Comput. Neuroscience 10, 281.

Hodgkin AL, Huxley AF (1952) A quantitative description of membrane current and its application to conduction and excitation in nerve. J. Physiol. 117: 500.

Hopfield JJ, Brody CD (2001) What is a moment? Transient synchrony as a collective mechanism for spatiotemporal integration. Proc. Natl. Acad. Sci. USA. 98: 1282–1287.

Hoppensteadt FC, Izhikevich EM (1998) Thalamo-cortical interactions modeled by weakly connected oscillators: Could the brain use FM radio principles? Biosystems. 48: 85–94.

Izhikevich EM (2000) Neural Excitability, spiking, and bursting. International. Journal of Bifurcation and Chaos. 10: 1171–1266.

Hounsgaard J, Kiehn O (1989) Serotonin-induced bistability of turtle motoneurones caused by a nifedipine-sensitive calcium plateau potential. J. Physiol. 414: 265–282.

CONTENT is available at ftp://ftp.cwi.nl/pub/CONTENT.

Lechner H, Baxter D, Clark C, Byrne J (1996) Bistability and its regulation by serotonin in the endogenously bursting neuron R15 in Aplysia. J. Neurophysiol. 75: 957.

Marder E, Calabrese RL (1996) Principles of rhythmic motor pattern generation. Physiol. Rev. 76: 687.

Marder E, Abbott L, Turrigiano G, Liu Z, Golowasch J (1996) Memory from the dynamics of intrinsic membrane currents. Proc. Natl. Acad. Sci. USA **26–93**(24), 13481.

Opdyke CA, Calabrese RL (1994) A persistent sodium current contributes to oscillatory activity in heart interneurons of the medicinal leech. J. Comp. Physiol. 175: 781–789.

Pontryagin LS, Rodygin LV (1960) Periodic solution of a system of ordinary differential equations with a small parameter in the terms containing derivatives. Sov. Math. Dokl. 1: 611–614.

Rinzel J, Ermentrout B (1989) Analysis of neural excitability and oscillations. In: C. Koch and I. Segev, eds., Methods of Neural Modeling: From Synapses to Networks. MIT Press, pp. 135–169.

Rowat PF, Elson RC (2004) State-dependent effects of Na channel noise on meuronal burst generation, J. of Computational Neuroscience 16: 87–112.

Schwarz C, Thier P (1999) Binding of signals relevant for action: Towards a hypothesis of the functional role of the pontine nuclei. Trends Neurosci. 22: 443–451.

Shilnikov AL, Cymbalyuk G (2005) Transition between tonic spiking and bursting in a neuron model via the blue-sky catastrophe. Phys Rev Letters 94: 048101.

Shilnikov AL, Calabrese RL, and Cymbalyuk GS (2004) Mechanism of bi-stability: Tonic spiking and bursting in a neuron model. Phys. Rev. E. (submitted).

Shilnikov AL, Calabrese RL, Cymbaluyk G (2005) How a neuron model can demonstrate coexistence of tonic spiking and bursting? Neurocomputing (accepted for publication).

Shilnikov LP, Shilnikov AL, Turaev DV, Chua LO (1998, 2001) Methods Qualitative Theory in Nonlinear Dynamics, Volumes I and II. World Sci. Publ.

Shilnikov AL, Rulkov NF (2003) Origin of chaos in a two-dimensional map modelling spiking-bursting neural activity. Bifurcations and Chaos 13(11): 3325–3340.

Shilnikov AL, Rulkov NF (2004) Subthreshold oscillations in a map-based neuron model. Physics Letters A328: 177–184.

Shilnikov AL, Shilnikov LP, Turaev DV (2004) Mathematical aspects of classical synchronization theory, Tutorial. Bifurcations and Chaos 14(7): 2143–2160.

Terman D (1992) The transition from bursting to continuous spiking in an excitable membrane model. J. Nonlinear Science 2, 135–182.

Turrigiano G, Marder E, Abbott L (1996) Cellular short-term memory from a slow potassium conductance. J. Neurophysiol. 75: 963.

Vinogradova OS. (2001) Hippocampus as comparator: Role of the two input and two output systems of the hippocampus in selection and registration of information. Hippocampus. 11(5): 578–598.

Wang XJ (1993) Genesis of bursting oscillations in the Hindmarsh-Rose model and homoclinicity to a chaotic saddle. Physica D 62: 263–274.